Journal of Structural Engineering Vol.49A(March 2003) JSCE

Strength Characteristics at Bent Portion of Continuous Fiber Flexible Reinforcement

Roshan Tuladhar*, Yasuhiko Sato**, Tamon Ueda***Akira Kobayashi****

* PhD candidate, Graduate School of Eng., Hokkaido University, Kita-ku, Sapporo, 060-8628
** Dr. of Eng., Research Associate, Graduate School of Eng., Hokkaido University, Kita-ku, Sapporo, 060-8628
*** Dr. of Eng., Associate Professor, Graduate School of Eng., Hokkaido University, Kita-ku, Sapporo, 060-8628
**** M. of Eng., General Manager, Structural Engineering Dept. Tow Sheet div., Nippon Steel Composite Co. Ltd.

The bent performance of Continuous Fiber Flexible Reinforcement (CFFR) as continuous shear reinforcement for concrete structures has been examined. Two different types of bent specimens were prepared. In the first type the strain characteristics past the bent portions were examined at different strain level with CFFR arranged continuous like in an actual column. In the second type, the strength of bent, rupture strain and loss past the bent portion were investigated under different main bar diameter, angle of bent and embedded length. The experimental results on the bent strength and loss across the bent are presented under different parameter for CFFR. In addition to usual radius of bent stated in the JSCE bent strength equation it seemed the angle of bent is also an influential factor governing the bent strength of continuous shear reinforcement.

Key Words: Flexible Shear Reinforcement, Bent Strength, Loss across Bent, CFFR

1. Introduction

Seismic design for reinforced concrete structure requires the huge amount of stirrup and intermediate stirrups to restraint lateral dilation of in-core concrete under seismic action. The demand for heavy provision of shear reinforcement has potential to induce great construction difficulties for arrangement and providing acute angle hooks. With the motive to overcome constructional workmanship errors an innovative form of continuous flexible shear reinforcement had been developed before[1]. It has been named Continuous Fiber Flexible Reinforcement, CFFR in short. CFFR is simply a collection of millions of carbon fibers in a long transparent plastic tube. The length can be tailored to the need. The system is highly flexible; therefore can be arranged to any desired shape prior to resin injection and hardening to form in-situ molded reinforcement. The property of CFFR is shown is Table 1. For efficient application of such a continuous flexible shear reinforcement mechanical anchorage is provided at the two extremities by highly expansive material in steel tube. CFFR is used as one piece continuous shear reinforcement. Unlike conventional steel stirrup it therefore has angle of inclination.

Table 1. Mechanical Property of CFFR

Area (mm^2)	Modulus (GPa)	Ultimate Strength (MPa)	Ultimate Strain (μ)	Tube Thickness (mm)
16.89^a	265	4132	15600	1

Note: ^{a}Cross Sectional Area of Carbon Fiber Only.

The CFFR has been used as shear reinforcement in addition to minimum amount of steel stirrup to large scale reinforced concrete column and tested under cyclic and reversed cyclic displacement reversals[2]. The failure mode of CFFR reinforced concrete piers have been reported as the rupture of CFFR at the bent portion due to localized stress concentration and its position is schematically shown in Fig. 1. But during member level experiment it was not possible to catch the rupture strength of CFFR at the bent portion. Moreover, the rupture of CFFR was found to happen at the bent portions

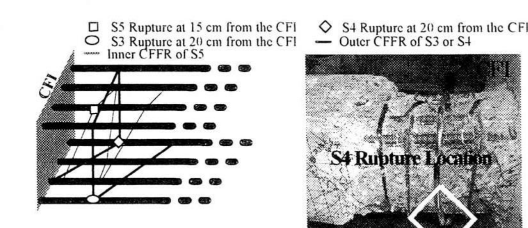

CFI = Column Footing Interface

S3, S4 and S5 are specimen numbers as in reference 2.

Fig. 1. Sketch of Ruptured Bent portions and a Column

which has some inclination rather than at the straight bents similar to steel stirrup. This led the authors to the importance of understanding the rupture strength of CFFR under various angles at bents. It is well known that the stress concentration at the bent is essentially affected by the radius of curvature of bent. The JSCE design equation of bent strength also includes the parameter of ratio of radius of bent to height of bent bar[3]. The CFFR is wound around the main reinforcing bar tightly before resin injection and therefore the radius of curvature of CFFR can be considered as related to diameter of main bar. In the column experiment, the CFFR is wound around the main bars forming inner and outer core. The rupture was found to be possible to happen in inner core CFFR or outer core CFFR (Fig. 1). It was thought that the distance of bent portion from the crack plane might influence the condition of stress at the bent portion due to difference in local slip at the bent portion.

In the same column experiments, strain gauges were attached in between two consecutive bent portions and force transfer characteristic at the bent portion was studied. Based on strain data of CFFR, it was found that the stress transfer across the bent portion of CFFR had tendency to become constant as the strain level increases in CFFR. Moreover, about 80% strain was also reported possible to be transferred through the bent portion. Such information is necessary to be incorporated in numerical analysis tool to simulate the behavior of CFFR more appropriately. In this study, loss across the bent portion of CFFR under different condition of angle of bent, bar diameter, strain level and embedded length of CFFR was also studied

2. Experimental Program

The detail of each specimen and parameters are stated in

Table 2 Specimen Details and Parameters

Specimen	Main Bar	No. of Bents	Consecutive Bent angles degree	Length in Concrete	
				before bent mm	after bent mm
C1-1	D13	5	29, 29, 0, 45, 45	250, 103, 210, 210, 270	103, 210, 210, 270, 210
C1-2	D25	5	29, 29, 0, 45, 45	250, 103, 210, 210, 270	103, 210, 210, 270, 210
C1-3	D25	4	29, 29, 0, 45	250, 103, 210, 70, 250	103, 210, 70, 250, 250
C2-1-0	D13	1	0	140	190
C2-1-20	D13	1	20	140	200
C2-1-45	D13	1	45	140	230
C2-2-0	D25	1	0	70	190
C2-2-20	D25	1	20	70	200
C2-2-45	D25	1	45	70	230
C2-3-0	D25	1	0	140	190
C2-3-20	D25	1	20	140	200
C2-3-45	D25	1	45	140	230

Table 2. Two different types of experimental specimens were prepared in this study and named C1 and C2 series. In the C1 series specimen, the CFFR were wound around the main bars like stirrups in the column but continuous. The typical experiment setup and dimensions for C1 series specimen is shown in Fig. 2. There were three specimens in C1 series. The arrangement of CFFR around the main bars in C1 series specimen is shown in Fig. 3. In case of C2 series experiment, CFFR were bent at the single main bar and clamped at the other extremities. There are all together 9 specimens of this type. Three specimens having same diameter or embedded-length was molded as a set of concrete specimen as shown in Fig. 4 for C2-3 specimens. The specimens are put over the base plate that has threaded holes at appropriate position to fix the specimen securely with pre-stressing bars. The base plate was fixed to the

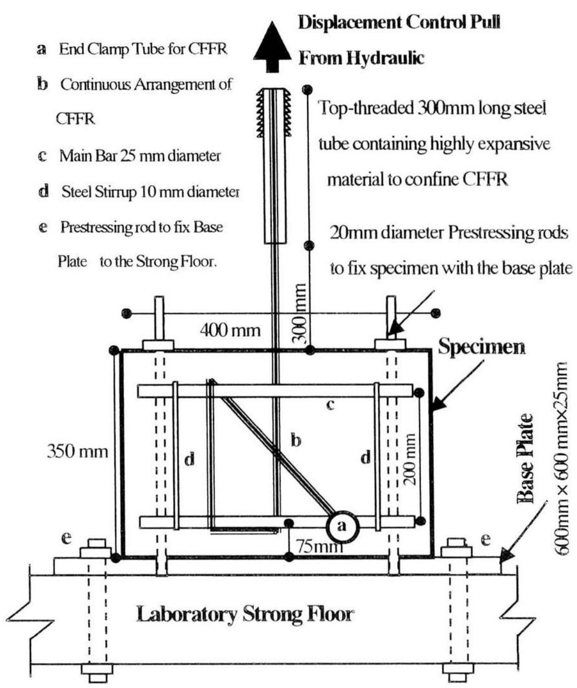

Fig. 2. Typical Experimental Setup for C1 series Specimen

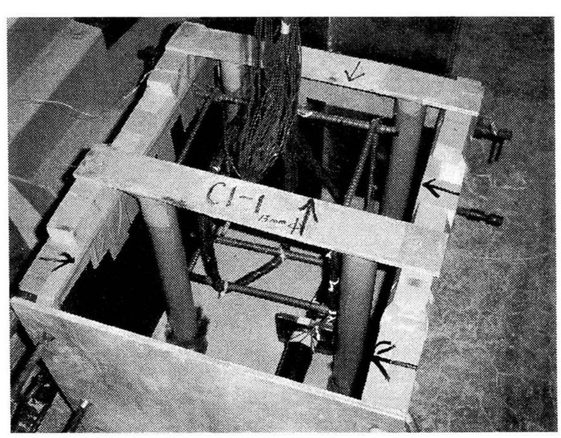

Fig. 3 .Arrangement of CFFR for C1-1

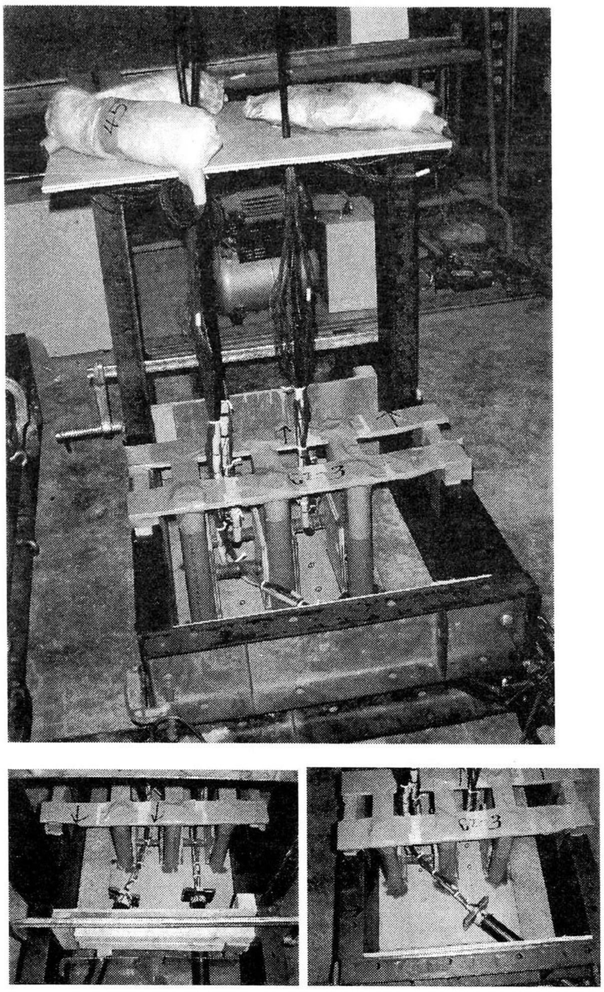

Fig. 4 Combining three sets of Specimens C2-3 in one mold (up). Top view of all three bent specimens and end clamps (bottom).

laboratory strong floor using 80kN pre-stressing force each in four pre-stressing bar. The specimen is located on the base plate such that the top portion of CFFR coming out of concrete block is at the center to fix to the loading machine. Displacement transducers were attached to the end of CFFR to examine its slip under big tensile load near rupture load. The slip of end CFFR was not exceeding to the third decimal point of a millimeter at the ultimate rupture state.

The top end of CFFR was anchored with highly expansive material used inside the steel tube 5 mm thick, 300 mm long and 43 mm internal diameter. It has threads on the outer surface to connect to the loading head of actuator through which the displacement was applied gradually. The loading path for all specimens is shown in Fig. 5. The other end of the CFFR was clamped using the steel tube partially embedded inside the concrete. This steel tube had flat square steel plate 5mm thick welded to the side of tube inside the concrete. It was intended to provide a bearing of end clamp tube against the concrete so that its movement under high tension can be restrained especially in the C2 series experiment where there is only one bent per

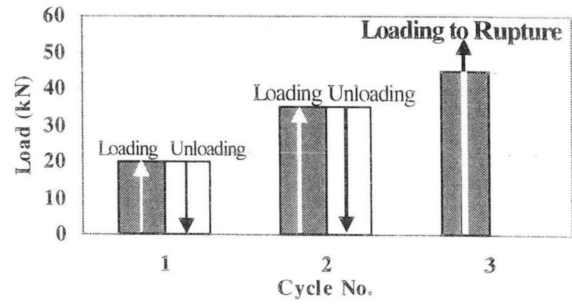

Fig. 5 Loading Path

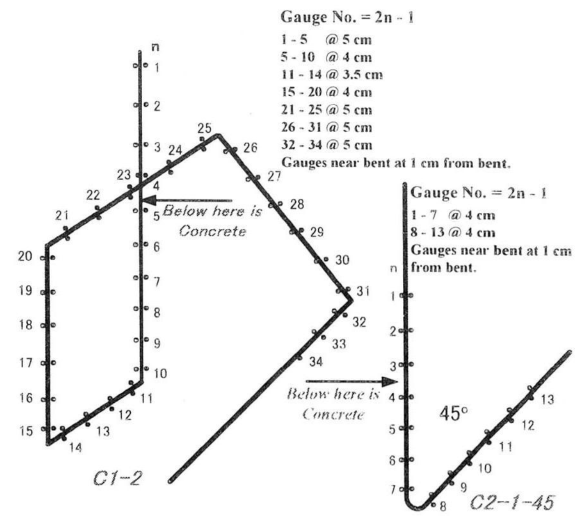

Fig. 6 Gauge Locations for C1-2 and C2-1-45

specimen. The CFFR is flexible initially. In order to produce CFFR of desired angle of bent around desirable bar diameter it was first wound around the big steel cage of appropriate size made of appropriate diameter of the main bar. Later after hardening of resin, CFFR was cut to appropriate dimension. The location of strain gauges is shown for typical specimens of C1 and C2 series in Fig. 6. There are two strain gauges attached at each location.

3. Strength of Bent

Basic stress analysis calculations assume that the element has a uniform section and no irregularities. Bents at the corners of shear reinforcement represents an abrupt change in section and shape. Such a discontinuity changes the stress distribution in the vicinity of the bents. The distribution of stress at or near the bent is complex over the section. Such irregular features cause local increase of stress at the bents referred to as stress concentration or stress raisers. The stress raisers are the points of weakness where the stress overcomes the fiber's local tensile strength and fracture originates. The exact theoretical solution derived for pure bending of curved bars [4] cannot be directly applied. The usual engineering practice to represent the stress localization is to define a stress concentration factor or bent strength ratio. Bent strength ratio is here defined as the ratio of average stress of the fibers in the original cross section nearest to the bent section to the unconfined tensile strength of the fibers in straight portion. The bent strength ratio calculated with the observed average strain near the bent at the rupture condition is compared for the different parameters in Table 3.

3.1 Characteristics of Strain measured near the bent

The average strain at a section measured farther from the bent portion has tendency to converge whereas that near the bent portion has irregular tendency. Fig. 7 shows the maximum strain at a section normalized by the average strain at the section vs. average strain at different positions of C1-2 for the part of CFFR embedded inside the concrete up to the first bent. Fig. 8 shows the recorded strain data at those positions at 20kN and 35kN load level. The difference in recorded strain near the bent portion at the same section is very large compared to farther straight portions. This shows that the assumption of linear strain

Table 3 Bent Strength ratio of CFFR

Specimen	Bent Strength ratio	Bent Angle	Re-bar Dia. mm	Embed. Length mm	Restraint*	CFFR ht. at bent mm
C1-1	0.555	29°	13	250	1	
C1-2	0.499	29°	25	250	1	
C1-3	0.560	29°	25	250	1	
C2-1-0	0.709	0°	13	140	0	4.4
C2-1-20	0.662	20°	13	140	0	4.35
C2-1-45	0.594	45°	13	140	0	4.6
C2-2-0	0.821	0°	25	70	0	4.65
C2-2-20	0.505	20°	25	70	0	4.6
C2-2-45	0.728	45°	25	70	0	4.7
C2-3-0	0.790	0°	25	140	0	
C2-3-20	0.713	20°	25	140	0	
C2-3-45	0.655	45°	25	140	0	

*Restraint is shown 1 for column like condition and 0 for mechanical clamping

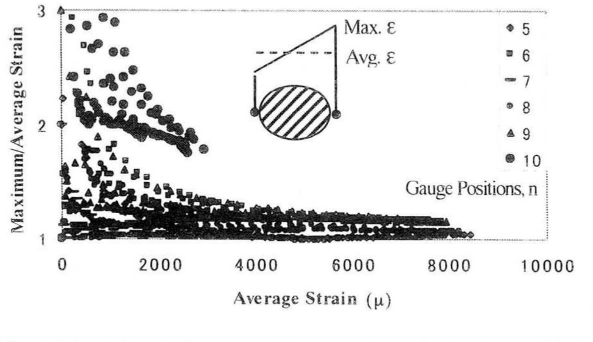

Fig. 7 Normalized Maximum Strain vs Average Strain for C1-2

variation across the section cannot always be true near the bent portion. In the theory of elasticity, assuming the cross sections of a bar remain plane during the bending, the distribution of normal stresses over any cross section had been shown to follow a hyperbolic law[4]. Such an assumption is valid if the height of the bent bar is not small compared to the radius of the bent. In case of CFFR, the height of CFFR at the bent portion is smaller because the CFFR is tightly wound around the main bar and in doing so the height reduces. The CFFR of C2-1 and C2-2 specimens after the experiment were recovered. The plastic tube at the bent portion was cut and the average depth of CFFR below the location of main bar was measured using a vernier caliper and shown in last column of Table 3. Below the main bar location the resinated fibers are damaged completely as shown in Fig. 9.

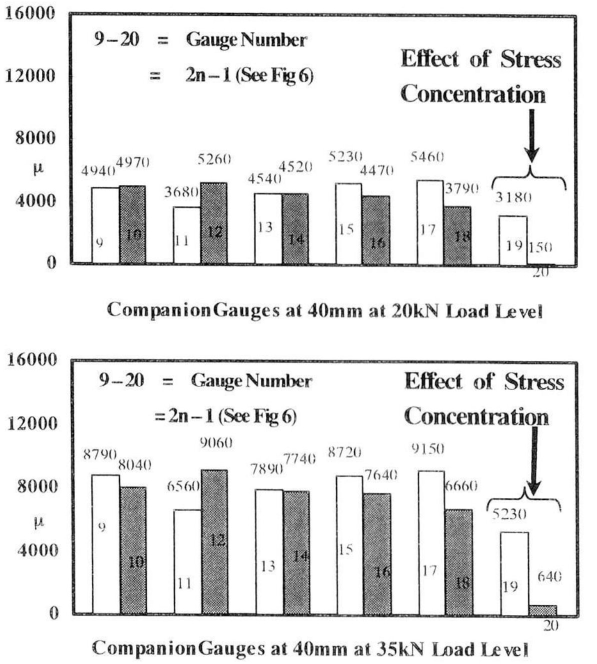

Fig. 8 Strain development for C1-2 at each gauge number

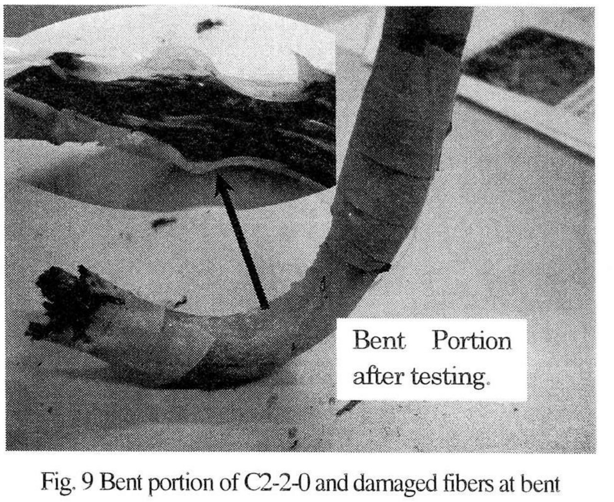

Fig. 9 Bent portion of C2-2-0 and damaged fibers at bent

3.2 Bent Strength for Different Bent Angle

The angle of bent of CFFR (θ in Fig. 10) is defined as the angle to inclination relative to usual leg of direction of stirrup. This angle of bent is the typical of continuous shear reinforcement. C2 series experimental data corresponds to three different angles of bent for different diameter of main bar and embedded length in concrete.

Fig. 10 shows the comparison of bent strength ratio for specimens C2-1, C2-2 and C2-3 all of which have three different angles of bent but different diameter of bar or different embedded length. Except the 20^{o} case for C2-2 all other specimens show decrease in bent strength ratio with increase in angle of bent. The reason why C2-2-20 shows relatively lower strength is not clear at this moment. The average gradient of bent strength ratio with angle of bent, θ, in radian for 13mm and 25 mm diameter bars are respectively 0.145/radian and 0.177/radian. With the increase in angle of bent of CFFR, the contact area of CFFR with the main bar increases. The reaction force from the main bar acts to the CFFR fibers on this contact surface. With the introduction of angle of bent, the fibers at bent are twisted in addition to tension. When the fibers at the bent portion are only under tensile forces, the bending stress distribution across the depth of CFFR can be almost uniform along the CFFR section. When the angle of bent of CFFR increases, this bending stress distribution no longer becomes uniform across the CFFR section. This induces additional stress concentration in addition to stress concentration at the bent portion of common 0^{o} case. Consequently, the bent strength ratio reduces as angle of bent of CFFR increases.

3.3 Bent Strength for Different Bar Diameter

Fig. 11 shows the comparison of bent strength of specimens C2-1 and C2-3 which have same embedded length and only the difference is diameter of main bar. The bent strength ratio of CFFR has tendency to be increased with the increase in diameter of the main bar. This can be explained by the fact that CFFR is wound around the main bar tightly unlike curved placement with fixed radius of bent for steel stirrup. So the radius of bent for CFFR is the sum of radius of main bar and the half the thickness of CFFR at the bent portion (Fig 12). Therefore the stress concentration at the bent portion can be expected smaller and consequently bent strength ratio can have tendency to increase with increase in diameter of main bar.

3.4 Bent Strength for Different Embedded Length

Fig. 13 shows the comparison of bent strength of specimens C2-2 and C2-3 which have same main bar diameter but the only difference is the length of CFFR inside concrete up to the bend portion. Except the specimen C2-2-20, there is tendency that the bent strength ratio can decrease with increase in embedded length. It is expected that when the diagonal crack plane is nearer to the bent portion, the local slip of CFFR at the bent portion will influence on the bent strength.

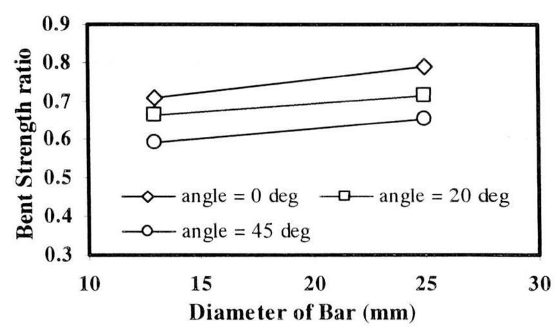

Fig. 11 Bent Strength vs Diameter of main Bar

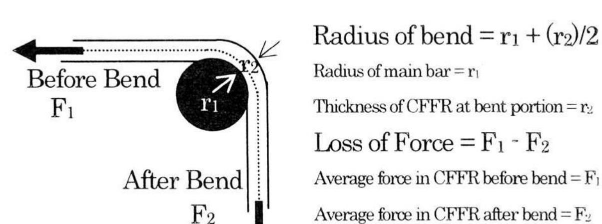

Fig. 12 Radius of Bend and Loss of Force

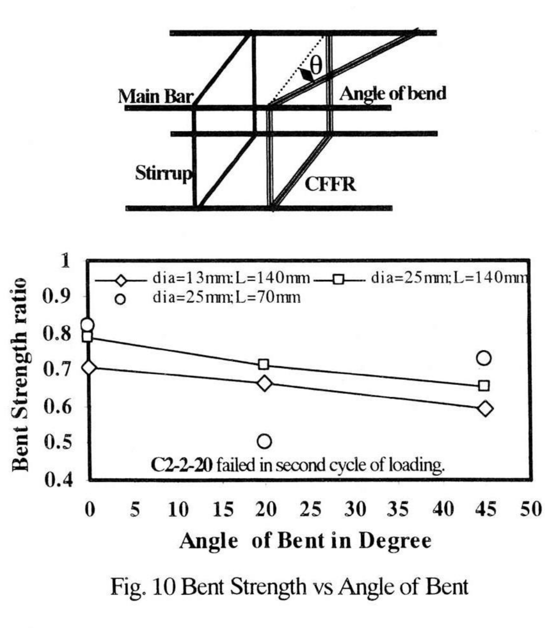

Fig. 10 Bent Strength vs Angle of Bent

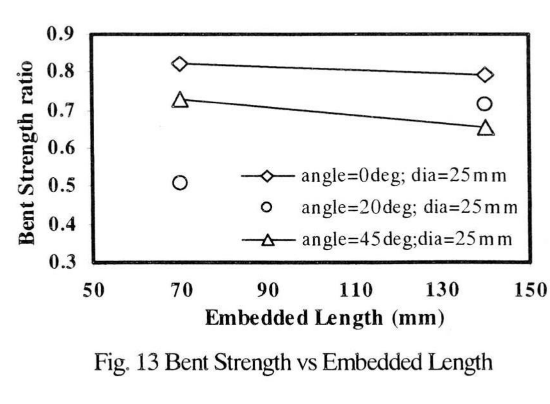

Fig. 13 Bent Strength vs Embedded Length

3.5 Bent Strength for Different Restraint Condition

In Table 3 it can be seen that the bent strength of CFFR is smaller for C1 series specimens than that of C2 series except for C2-2-20. The experimental parameters were not designed to study the difference in bent strength due to restraint condition. In C1 series specimen angle of bent is 29° and in C2 series angles 20° and 45° are nearer to 29°. The embedded length in C1 series is 250mm and in C2 series length of 140mm is the nearest to 250mm. Fig. 14 shows the comparison of bent strengths of C1 series experiment with that of 45° and 20° cases of C2-1 and C2-3 separately. In the Fig. 14 the condition of restraint for C1 series is represented by 1 and that of C2 series by 0. In the first figure the fraction of bent strength for two different restraint conditions are respectively 93%, 85% and 76%. In the second figure the fraction, it is respectively 83%, 78% and 70%. The mechanical restraint can reduce the local slip at the bent portion. Also the embedded length is higher in C1 series which might have influence on the slip at the bent portion leading to initiation of failure at lower stress level.

3.6 Comparisons of Bent Strengths to JSCE Prediction

The JSCE has proposed the design strength of bent portion of Continuous Fiber Reinforcing Material[3]. According to it, the ratio of characteristic value of strength of bent portion to the characteristic value of unconfined tensile strength, η, is given by the regression equation as:

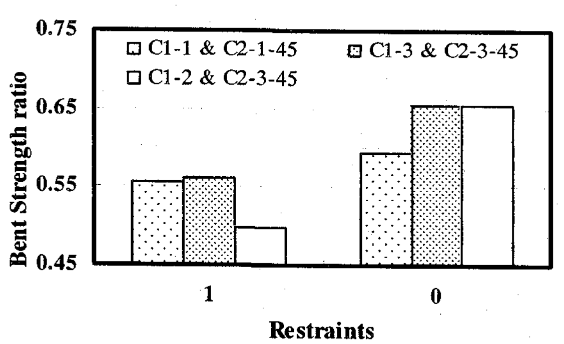

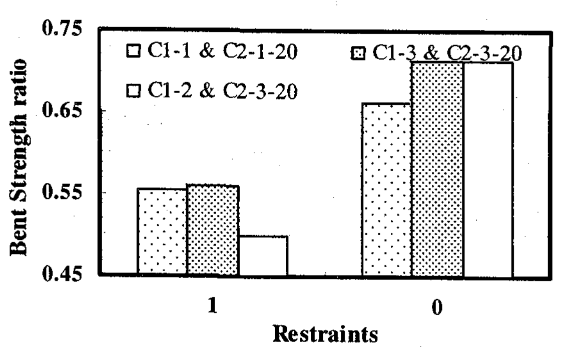

Fig. 14 Bent Strength for different restraint conditions

$$\eta = 0.09\frac{r}{h} + 0.3 \qquad (1)$$

where, r = internal radius of the bent
h = cross sectional height of CFRM

The cross sectional height of CFFR at the bent portion is not the same as diameter of the CFFR. It is about 45% of it as noted in Table 3 as measured average values. The r/h parameter for different bent specimens is calculated and stated in Table 4. The JSCE bent strength is calculated for condition of CFFR at bent as 50% of the diameter of CFFR (10mm) and shown in Fig. 15. The JSCE strength equation can predict the bent strength to safer side with only a function of r/h parameter; however it seemed some other parameter such as angle of bent should also be included for one-piece continuous shear reinforcement.

4. Loss across the bent

When force is transferred across the bent portion, there is some frictional loss at the bent-portion (Fig 12). The loss of force in the CFFR first straight portion inside the concrete compared to that in the air is small as shown in Fig. 16 for

Table 4 Experiment and JSCE Bent Strengths

Specimen	Expt. Bent Strength	r/h*	JSCE Bent Strength for flatness of CFFR as 50%
C1-1	0.555	0.65	0.417
C1-2	0.499	1.25	0.525
C1-3	0.560	1.25	0.525
C2-1-0	0.709	0.65	0.417
C2-1-20	0.662	0.65	0.417
C2-1-45	0.594	0.65	0.417
C2-2-0	0.821	1.25	0.525
C2-2-20	0.505	1.25	0.525
C2-2-45	0.728	1.25	0.525
C2-3-0	0.790	1.25	0.525
C2-3-20	0.713	1.25	0.525
C2-3-45	0.655	1.25	0.525

*r is taken as radius of main bar and h as diameter of CFFR here.

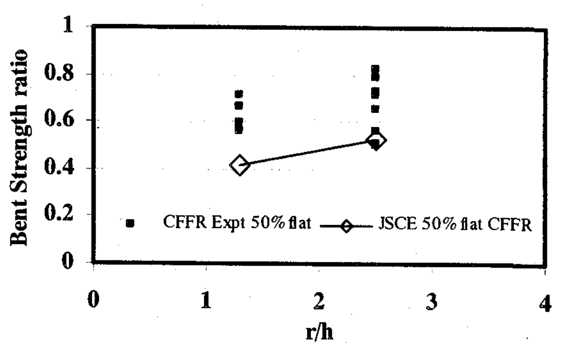

Fig. 15 Experiment and JSCE Bent Strengths

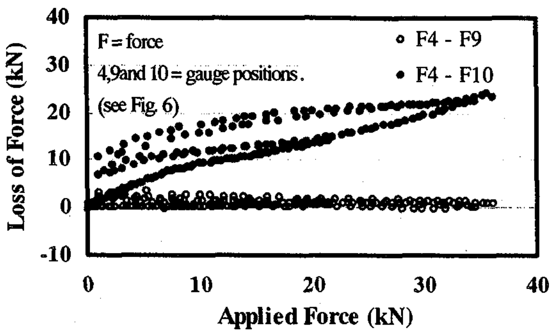

Fig. 16 Total force loss in CFFR embedded in concrete

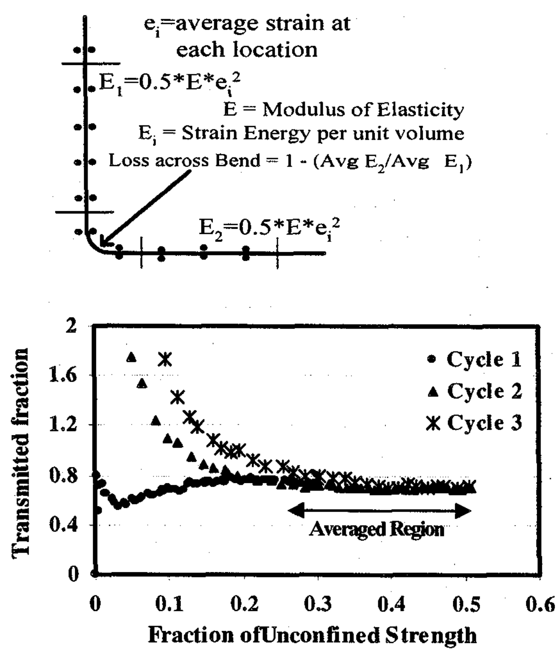

Fig.17 Fraction of Energy Transmitted across the first bent of C1 -2

Table 5 Loss of Energy across the bents

Specimen	Diameter mm	Angle degree	Length mm	$\varepsilon/\varepsilon_m$ *	Restraint	Transferred Fraction	Loss
C1-1	13	29	250	0.55	1	0.82	0.18
	13	29	100	0.52	1	0.48	0.52
	13	0	210	0.47	1	0.47	0.53
	13	45	210	0.28	1	0.41	0.59
	13	45	270	0.22	1	0.50	0.50
C1-2	25	29	250	0.51	1	0.71	0.29
	25	29	100	0.50	1	0.31	0.69
	25	0	210	0.42	1	0.37	0.63
	25	45	210	0.23	1	0.37	0.63
	25	45	270	0.14	1	0.56	0.44
C1-3	25	29	250	0.60	1	0.70	0.30
	25	29	100	0.58	1	0.42	0.58
	25	0	210	0.30	1	0.45	0.55
	25	45	70	0.30	1	0.54	0.46
C2-1-0	13	0	140	0.67	0	0.73	0.27
C2-1-20	13	20	140	0.70	0	0.70	0.30
C2-1-45	13	45	140	0.51	0	0.69	0.31
C2-2-0	25	0	70	0.84	0	0.75	0.25
C2-2-20	25	20	70	0.51	0	0.75	0.25
C2-2-45	25	45	70	0.71	0	0.71	0.29
C2-3-0	25	0	140	0.69	0	0.78	0.22
C2-3-20	25	20	140	0.80	0	0.75	0.25
C2-3-45	25	45	140	0.69	0	0.73	0.27

* attained strain divided by the uniaxial tensile strength

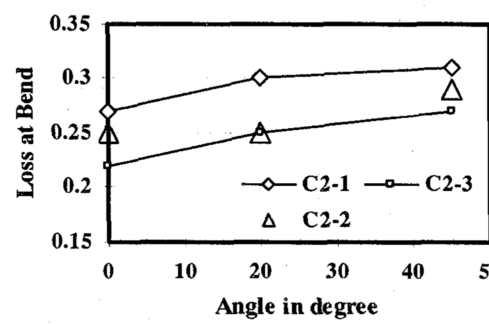

Fig. 18 Losses for different angle of bent

specimen C1-2 where embedded length is 250 mm. The reason why the loss calculated with the gauges nearest to the bent portion is very high is explained in the section 3.1 that nearest to bent portion the strain distribution across the section no longer remains linear. The strain measured at straight portions before the bent and after the bent can be utilized to quantify the loss at the bent portion. Ignoring other external forces in CFFR, the strain energy per unit volume is the second order function of measured strain. The average strain energy per unit volume in the straight part except near the bent portion was calculated and averaged. The average strain energy per unit volume of the straight part across the bent portion normalized by that before the bent portion means the fraction of energy transmitted across the bent portion. Therefore, one minus this fraction represents the loss across the bent portion.

Fig. 17 shows the typical fraction of strain energy transmitted across the bent portion for the first bent of specimen C1-2. It can be seen that the stable fraction of strain energy transmitted across the bent potion has tendency to shown more of less constant fraction at higher strain level. The average of the fraction of transmitted strain energy from where they nearly converge to the ultimate state is taken as the fraction of transmitted energy across the bent portion. All the values of such average constant transmitted fraction of energy for all the bents with different parameters are listed in Table 5. Following discussions in relation to bent strength can be done:

4.1 Loss for different bent angle

In Fig. 18 except the C2-2-20, other specimens of C2 series show the increase in loss at the bent portion with increase

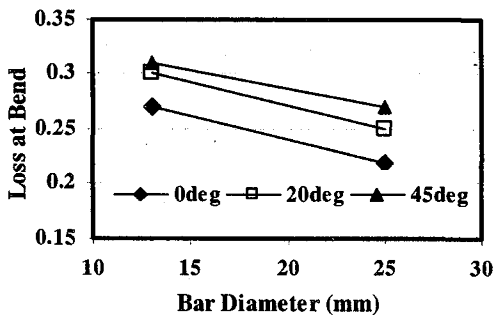

Fig. 19 Losses for different bar diameter

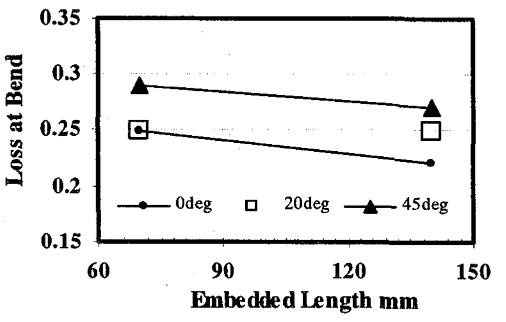

Fig. 20 Losses for different embedded lengths

in angle of bent. This trend is reverse of bent strength. This might mean that with increase in loss across the bent portion, the bent strength decreases.

4.2 Loss for different bar diameter

Fig. 19 shows comparison for C2-1 and C2-2 specimens. The loss at the bent portion decreases as the diameter of the bar increases. The trend is reverse of bent strength.

4.3 Loss for different embedded length

Fig. 20 for C2-2 and C2-3 shows that the loss at the bent portion has tendency to decrease with the increase in embedded length. This tendency is not reverse to that of bent strength.

4.4 Loss for different strain level

Fig. 21 shows all the cases listed in Table 5 for different ultimate strain level. It can be seen that for the second or other bents of C1 series specimens where strain level decreases, the loss is higher. In case of first bent or the only bents of C2 series specimens, the loss at the bent portion is lower.

5. Conclusions

Following conclusions can be drawn from this study:

1) Bent strength for continuous fiber shear reinforcement

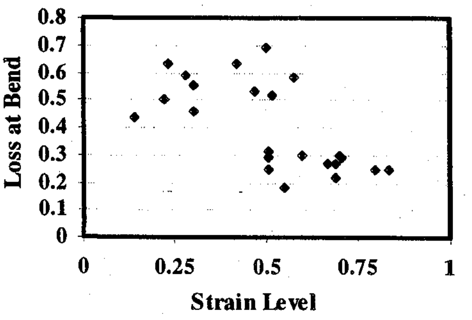

Fig. 21 Losses for different strain level

show relation with the angle of bent. It is seen that the bent strength ratio has tendency to decrease with the increase in angle of bent. The loss across the bent portion also has tendency to increase with angle of bent.

2) The bent strength of CFFR is higher for the greater diameter bar which follows the idea in JSCE design equation.
3) The bent strength seemed to be obtained higher in experiment with restraint ends using mechanical anchorage.
4) Loss across the bent portion has tendency to become stable at higher strain level and can explain the bent strength characteristics.

Acknowledgements

This study is the part of research supported by the Japanese Government (Monbusho) scholarship that is gratefully acknowledged. The assistance of graduate student Mr. Yoshinori Utsunomiya and others and laboratory supervisor Mr. Kimura Tsutomu is also acknowledged. The authors would also like to thank Prof. Yoshio Kakuta for valuable suggestions and advice.

References

1) Tomita, S., Kozaki, S., Sato, Y. and Kobayashi, A., A study on Continuous Fiber Flexible Reinforcement as shear reinforcement for concrete members, Transactions of the Japan Concrete Institute vol. 21, pp.235-240, 1999.
2) Tuladhar, R., Okubo, S., Sato, Y. and Kobayashi A., Deformational Characteristics of RC Columns with Continuous Fiber Flexible Reinforcement, the 8th East Asia Pacific Conference on Struct. Engg. and Const., Singapore no.1298(in CD).
3) Machida, A., Recommendation for Design and Construction of Concrete Structures using Continuous Fiber Reinforcing Materials, Concrete Engineering Series 23, JSCE.
4) Timoshenko, S.P. and Goodier, J.N., Theory of Elasticity, McGraw-Hill Book Company, pp. 71-74, 1970.

(Received September 13,2002)